Functional interaction between Sgs1 and Sod2 in the suppression of oxidative-damage-induced chromosomal rearrangements and mitochondrial abnormalities in *Saccharomyces cerevisiae*

Sonia Vidushi Gupta[a] *, Lillian Campos-Doerfler[a] and Kristina Hildegard Schmidt[a] *

[a] University of South Florida

* soniavidushi@usf.edu, kschmidt@usf.edu

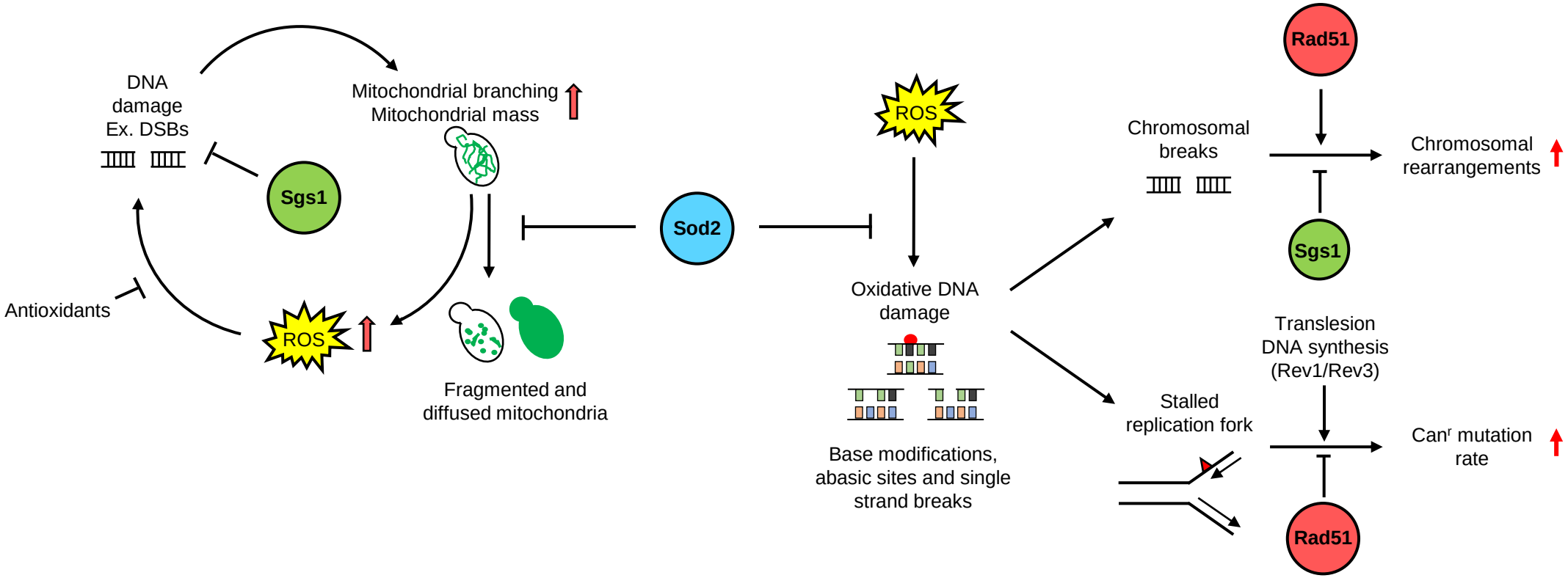

SILAC-based mass spectrometry reveals upregulation of ROS scavenging enzymes such as the mitochondrial superoxide dismutase Sod2 and thioredoxin peroxidase Tsa1

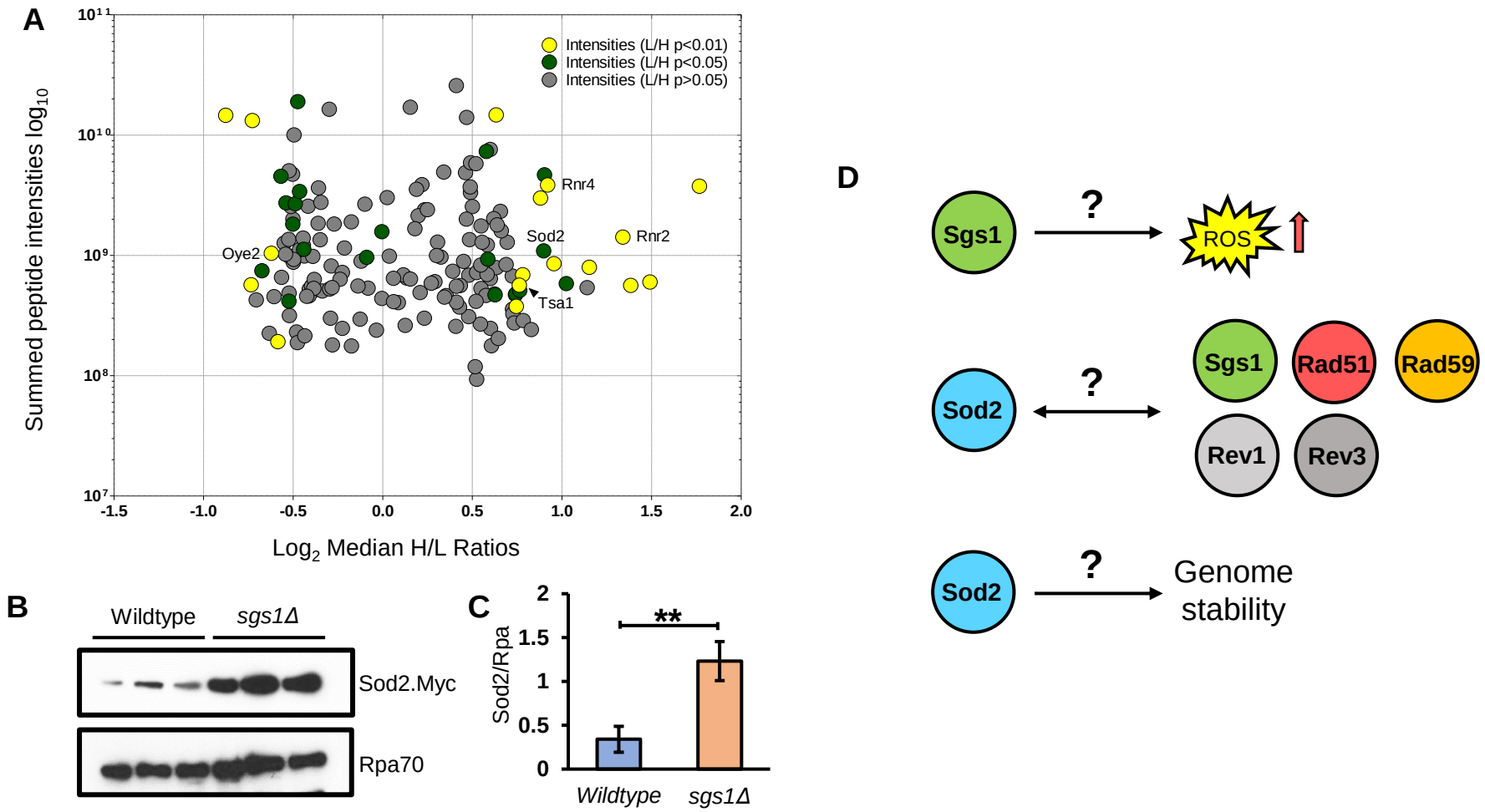

Figure 1 (A) Stable isotope labeling of amino acids in cell culture (SILAC)-based quantitative mass spectrometry from chromatin enriched fractions of biological triplicates of wild-type and *sgs1Δ* mutants. (B) Western blot analysis of Sod2.Myc expression levels in chromatin enriched fractions of wild-type and *sgs1Δ* mutants. Rpa70 was used as a loading control. (C) Quantification of Sod2.Myc expression levels compared to Rpa70 levels. (D) Overview of the research questions addressed in this study. All experiments were performed in triplicate and error bars represent the standard deviation. Statistical significance was determined with a Student's t-test and reported as * $p \leq 0.05$, ** $p \leq 0.01$, *** $p \leq 0.001$, ns not significant.

Cells lacking Sgs1 have high ROS, high mitochondrial mass and increased ROS dependent DNA damage (double strand breaks)

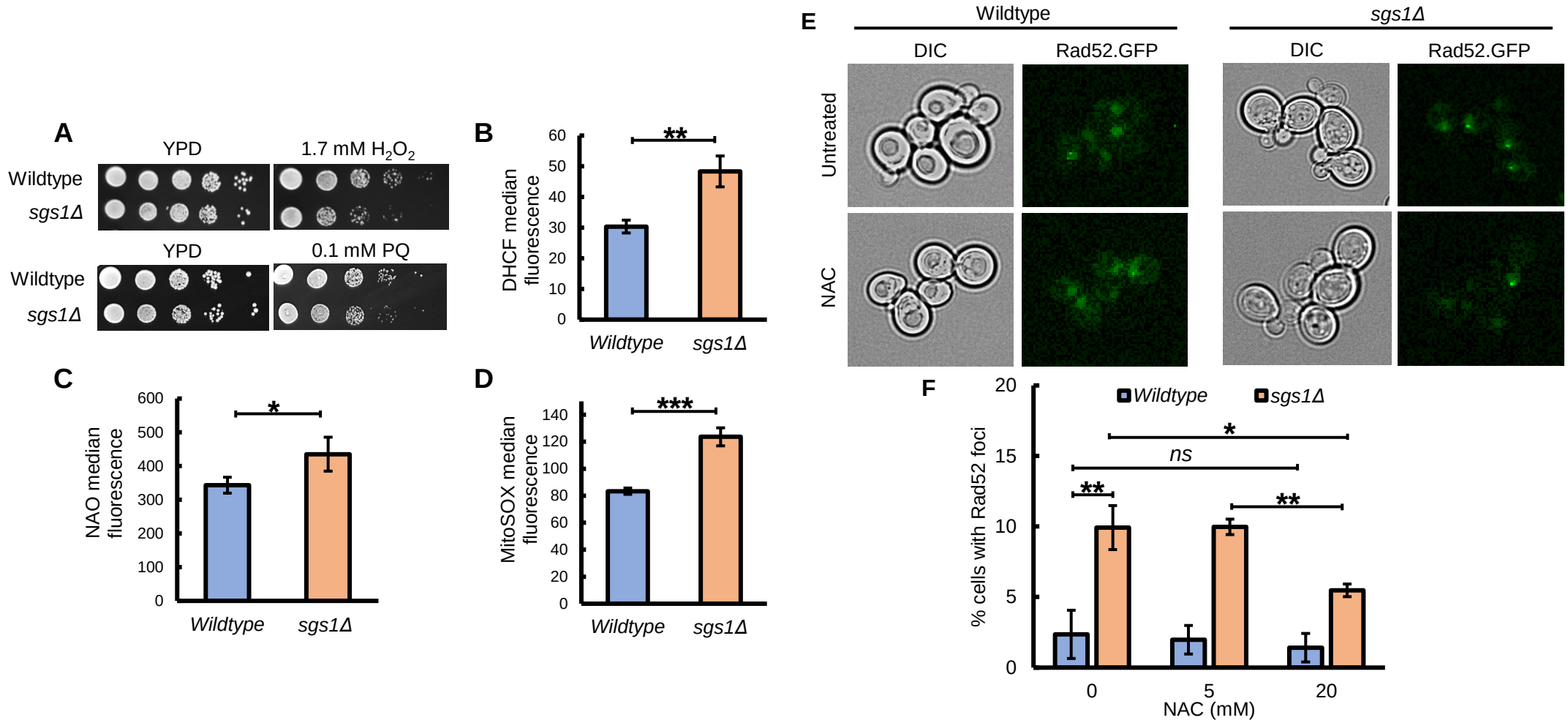

Figure 2 (A) Loss of *SGS1* sensitizes cells to oxidative damage by hydrogen peroxide (H_2O_2) and paraquat (PQ). (B) *sgs1Δ* mutants demonstrate a 40% increase in reactive oxygen species compared to wild-type, measured using the fluorescent dye 2', 7'-dichlorodihydrofluorescein diacetate (DHCF) via flow cytometry. (C) *sgs1Δ* mutants display a 20% increase in mitochondrial mass, measured using the fluorescent dye nonyl acridine orange (NAO) via flow cytometry. (D) *sgs1Δ* mutants display a 33% increase in mitochondrial superoxide content, measured using MitoSOX Red fluorescent dye via flow cytometry. (E) The percentage of cells with Rad52 foci were measured with fluorescence microscopy. Representative cells are shown. (F) Quantification of Rad52 foci in cells treated with varying amounts of the antioxidant *N*-acetyl-L cysteine (NAC). Statistical significance was determined with a Student's t-test and reported as * $p \leq 0.05$, ** $p \leq 0.01$, *** $p \leq 0.001$, ns not significant.

Sgs1 and Sod2 suppress mitochondrial abnormalities and inherent DNA damage promotes mitochondrial branching in cells lacking Sgs1

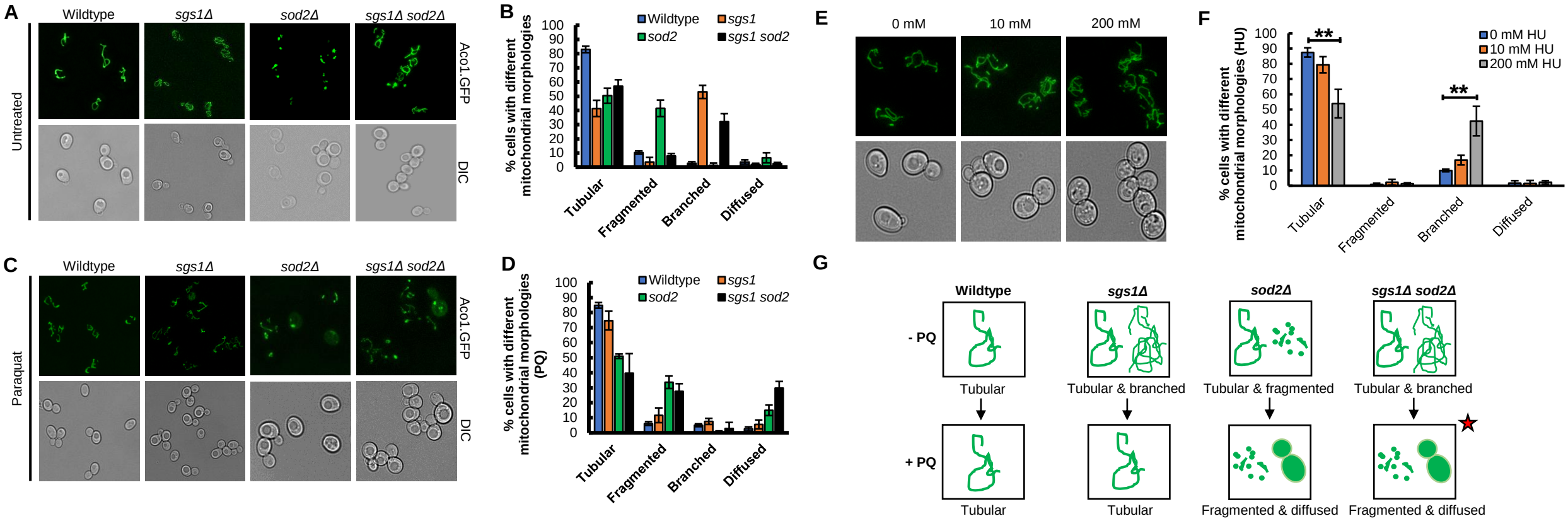

Figure 3 (A) Representative images demonstrating different mitochondrial morphologies in wild-type and mutant cells under untreated conditions and (B) quantification of the same. (C) Representative images demonstrating different mitochondrial morphologies in wild-type and mutant cells under PQ treated conditions and (D) quantification of the same. (E) Mitochondrial morphology in wild-type cells exhibits increased branching when exposed to increasing concentrations of DNA damaging agent hydroxyurea and (F) quantification of the same. (G) An illustration of the effect of PQ on mitochondrial morphology in various mutants. Star signifies that the respective phenotypes are more abundant compared to *sod2Δ*. Statistical significance was determined with a Student's t-test and reported as * $p \leq 0.05$, ** $p \leq 0.01$, *** $p \leq 0.001$, ns not significant.

Sgs1 suppresses Rad51-dependent chromosomal rearrangements of PQ-induced DNA breaks while translesion DNA synthesis promotes Can^r mutator phenotype in *sod2* mutants

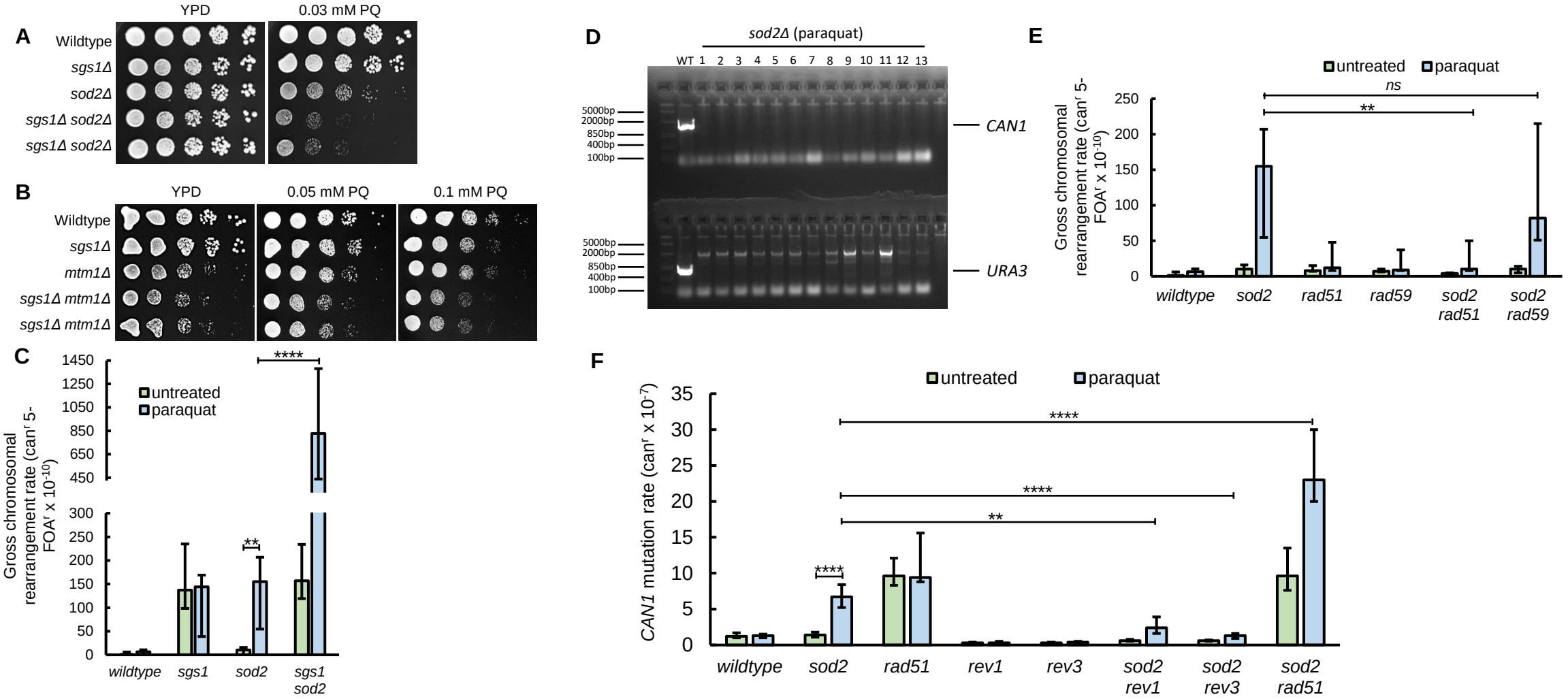

Figure 4 (A) *SGS1* is required for survival of *sod2Δ* mutants under PQ-induced oxidative stress. (B) The function of Sod2 in regard to Sgs1 is dependent on Mn-mediated Sod2 activity of redox regulation, controlled by Mtm1. (C) *sod2Δ* displays an increased GCR rate in the presence of PQ and *sgs1Δ* mutation causes a synergistic increase in the GCR rate of an *sod2Δ* mutant. (D) PCR amplification of *CAN1* and *URA3* genes from GCR clones of *sod2Δ* mutants treated with PQ demonstrates the occurrence of chromosomal breaks. (E) The GCR rate of *sod2Δ* mutants is Rad51-dependent. (F) The Can^r mutator phenotype of *sod2Δ* mutants is Rev1/Rev3 dependent whereas Rad51 suppresses mutagenesis. Median GCR and Can^r mutation rates are shown with 95% C.I. Statistical significance was determined with Mann-Whitney U test and reported as * $p \leq 0.05$, ** $p \leq 0.01$, *** $p \leq 0.001$, **** $p \leq 0.0001$, ns not significant.

Conclusions and future directions

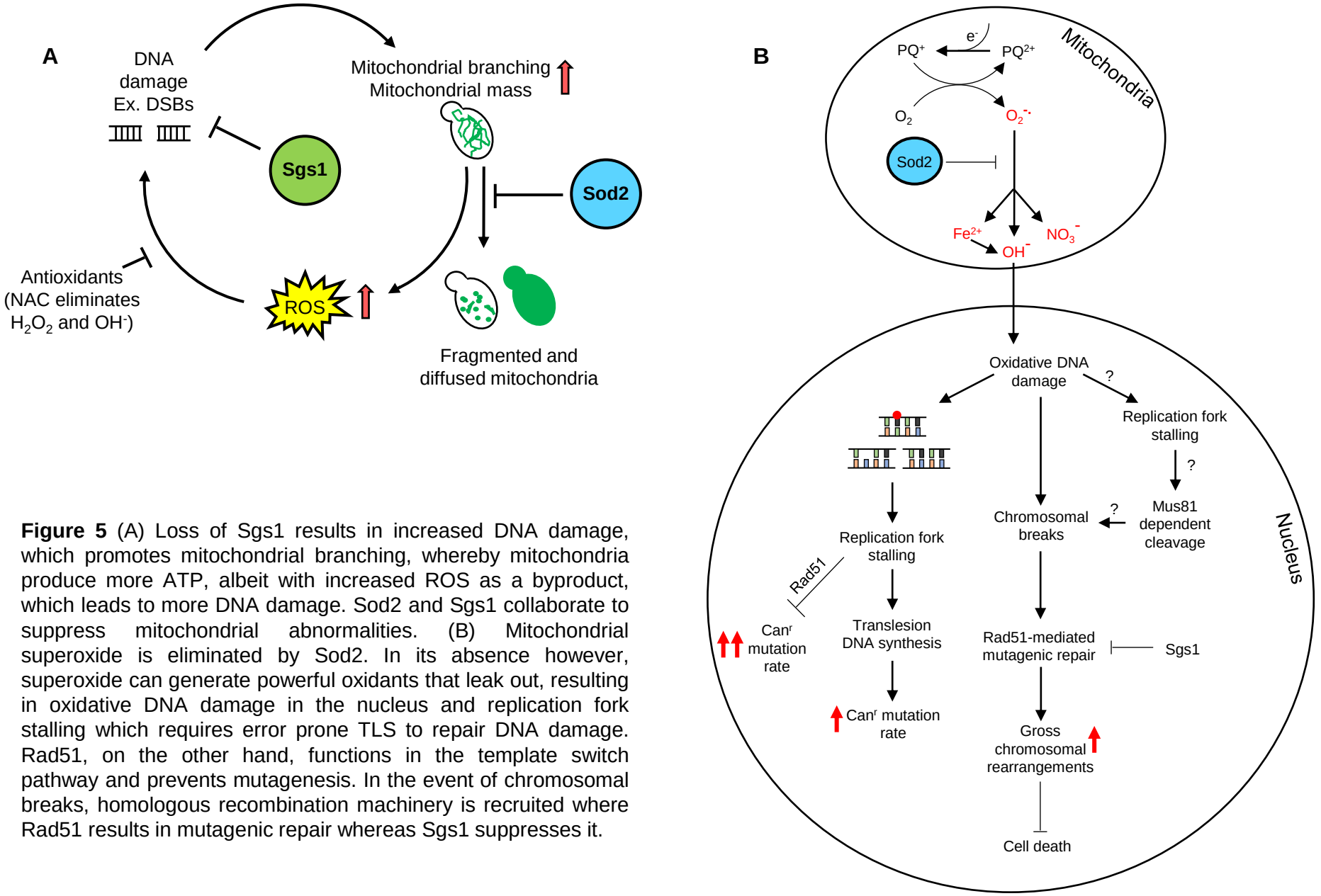

Figure 5 (A) Loss of Sgs1 results in increased DNA damage, which promotes mitochondrial branching, whereby mitochondria produce more ATP, albeit with increased ROS as a byproduct, which leads to more DNA damage. Sod2 and Sgs1 collaborate to suppress mitochondrial abnormalities. (B) Mitochondrial superoxide is eliminated by Sod2. In its absence however, superoxide can generate powerful oxidants that leak out, resulting in oxidative DNA damage in the nucleus and replication fork stalling which requires error prone TLS to repair DNA damage. Rad51, on the other hand, functions in the template switch pathway and prevents mutagenesis. In the event of chromosomal breaks, homologous recombination machinery is recruited where Rad51 results in mutagenic repair whereas Sgs1 suppresses it.

Future directions

- Are chromosomal breaks in *sod2* mutants generated directly via oxidative damage or through Mus81 dependent cleavage of stalled forks?
- What kinds of mutations does Rad51 suppress in *sod2* mutants?
- What kinds of mutations does translesion DNA synthesis generate in *sod2* mutants?